

Evaluating shape after-effects with radial frequency patterns

Nicole D. Anderson ^{*}, Claudine Habak, Frances Wilkinson, Hugh R. Wilson

Centre for Vision Research, York University, 4700 Keele Street, Toronto, Ont., Canada M3J 1P3

Received 14 September 2005; received in revised form 9 February 2006

Abstract

Mechanisms selective for complex shape are vulnerable to adaptation techniques historically used to probe those underlying performance in lower-level visual tasks. We explored the nature of these shape after-effects using radial frequency patterns. Adapting to a radial frequency pattern resulted in a strong and systematic after-effect of a pattern that was 180° out of phase with the adapting pattern. This after-effect was characterized as both a shift in the point of subjective equality and an increase in response uncertainty. The after-effect transferred across adapting pattern contrast and adaptor amplitude, suggesting an involvement from shape-specific mechanisms located at higher processing stages along the visual pathway. Moreover, our results suggested that the shift in the point of subjective equality was guided by global processing mechanisms, whereas the increase in uncertainty reflected activity from local processing mechanisms. Together, these results suggest that shape-specific after-effects reflect gain control processes at various stages of processing along the ventral pathway.

© 2006 Elsevier Ltd. All rights reserved.

Keywords: Shape after-effects; Adaptation; Form vision; Shape perception; Shape processing

1. Introduction

Adaptation techniques have proven to be a valuable tool for researchers concerned with the mechanisms that support visual processes. Selective adaptation has been applied in a variety of low-level feature domains such as contrast (Blakemore & Campbell, 1969; Greenlee & Heitger, 1988; Pantle & Sekuler, 1968; Wilson & Humanski, 1993), orientation (Campbell & Maffei, 1971; Gibson & Radner, 1937), and spatial frequency (Blakemore, Nachmias, & Sutton, 1970; Blakemore & Sutton, 1969), to elucidate the response characteristics of the mechanisms that support these percepts. More recently, research has focused on selective adaptation with naturalistic patterns in an attempt to understand the mechanisms that subservise complex object processing (for a review, see (Webster, 2004)). Adapting to a particular face identity, for example, induces a strong and systematic shift in perception that is identity-specific, suggesting independent neural population codes for differ-

ent face identities (Anderson & Wilson, 2005; Leopold, O'Toole, Vetter, & Blanz, 2001). Examples such as these illustrate how selective adaptation is a powerful technique for uncovering underlying neural response properties at a variety of different processing levels using purely behavioural methods.

Given the recent interest in complex object after-effects, surprisingly less attention has been given to adaptation effects for simple shape features. Most current models of object processing propose a processing hierarchy in pattern vision along the ventral processing stream, where outputs from lower-level processing mechanisms are integrated at subsequent stages to yield progressively more complex response profiles. While neurons in visual area V1 are selective for basic pattern features, such as orientation and spatial frequency (DeValois & DeValois, 1988; Hubel & Wiesel, 1968), neurons in visual area V4 are selective for more complex pattern features, such as curvature and relative position (Gallant, Braun, & Van Essen, 1993; Gallant, Connor, Rakshit, Lewis, & Van Essen, 1996; Kobatake & Tanaka, 1994; Pasupathy & Connor, 1999; Pasupathy & Connor, 2001). Responses from low-level discrete filters

^{*} Corresponding author.

E-mail address: anderson@hpl.cvr.yorku.ca (N.D. Anderson).

must therefore be combined to yield more complex feature representations at intermediate stages of visual processing. Moreover, V4 neurons respond to a larger region of visual space than neurons in V1, suggesting that local information from earlier filters is pooled over space to provide larger effective receptive fields at progressively higher stages along the visual hierarchy (Desimone & Schein, 1987). Following this pattern of hierarchical integration, neurons in high-levels of the ventral stream (i.e., inferotemporal cortex (IT)), tend to be highly selective for complex shapes such as faces, and are largely size and position invariant (Brincat & Connor, 2004; Kobatake & Tanaka, 1994). Again, this indicates that information from intermediate stages of processing is integrated in higher processing levels. Most adaptation paradigms to date have been designed to probe mechanisms at low-levels or high-levels of shape processing, but less is known about the nature of after-effects induced at intermediate stages of shape processing. Given the importance of intermediate processing mechanisms in the transformation of discrete local responses to complex global percepts, understanding the nature of these intermediate mechanisms is essential to our understanding of shape processing. Behaviourally, selective adaptation is an ideal tool to promote this understanding.

While after-effects related to complex features and simple shapes have been known to exist for some time (Gibson, 1933; Kohler & Wallach, 1944), the idea that these after-effects reflect activity from global shape-selective mechanisms has only more recently been proposed. Regan and Hamstra (1992) demonstrated that adapting to rectangles and/or ellipses resulted in the percept of a shape that was elongated along the opposite axis. This after-effect transferred across size and shape, providing evidence for a mechanism that responds purely to the aspect ratio of the stimulus. Suzuki and Cavanagh (1998) also demonstrated an axial after-effect that transferred across shape (from line to circle) that was position invariant. Finally, Suzuki (2001, 2003) presented evidence that shape after-effects induced with concave vs. convex figures are independent of adaptor contrast and dependent on attention. Size invariance, position invariance, contrast independence, and attentional dependence are all characteristic of global object processing mechanisms, providing strong evidence that these tasks are probing mechanisms that are responsible for processing global aspects of shape. However, none of these studies investigated after-effects induced with global curvature, an important shape characteristic. Discrimination thresholds for shapes defined in terms of geometric curvature are reduced after adaptation in a shape-specific manner (Alter & Schwartz, 1988). The nature of the perceptual after-effect after curvature adaptation, however, remains unknown.

In the present experiments, we evaluated shape after-effects using radial frequency patterns. Radial frequency patterns are narrowband forms in spatial frequency that define shape purely in terms of curvature deformation from a circle (Wilkinson, Wilson, & Habak, 1998). Given the

precise control that one has over the geometry of the form, these stimuli present themselves as excellent tools for investigating shape after-effects on perceived curvature. In our task, subjects identified the phase of a radial frequency pattern after adapting to a pattern that was either in-phase with or anti-phase to the test pattern. We found that adapting to a radial frequency pattern induced a strong and systematic after-effect of a radial frequency pattern that was anti-phase to the adapting pattern. Performance after adaptation was characterized by both a shift in the point of subjective equality and an increase in response uncertainty. The after-effect was independent of adapting contrast, suggesting that it reflected activity from mechanisms beyond those responsible for contrast gain control. The after-effect was also elicited by shapes with varying curvature amplitudes, suggesting that the after-effect partially reflects activity from mechanisms that process geometric shape independent from amplitude. Adapting to a different sized pattern induced a shift in the point of subjective equality without a change in response uncertainty. Conversely, adapting to a pattern with a different geometry did not induce a shift in the point of subject equality, but resulted in an increase in response uncertainty. Together, these results suggest that adapted mechanisms responsible for processing global stimulus features are responsible for the perceptual shift after adaptation, whereas adapted mechanisms responsible for processing local features are responsible for the reduction in certainty after adaptation.

2. General methods

2.1. Stimuli

We used radial frequency patterns (Wilkinson et al., 1998) to evaluate the effect of adaptation on shape processing. Radial frequency patterns are geometric patterns in which the contour is sinusoidally modulated from a base circle. In our experiments, the cross-sectional luminance profile of the base circle follows the fourth derivative of a Gaussian, such that:

$$D4(r) = C \left[\left(1 - 4 \left(\frac{r - r_{\text{mean}}}{\sigma} \right)^2 + \frac{4}{3} \left(\frac{r - r_{\text{mean}}}{\sigma} \right)^4 \right) \times e^{-\left(\frac{r - r_{\text{mean}}}{\sigma} \right)^2} \right], \quad (1)$$

where r is the radius of the base circle, C is the contrast, and σ determines the peak spatial frequency. Unless otherwise noted, r was held constant at 1° , the contrast of the radial frequency patterns was set to 90% and the peak spatial frequency was 8.0 cpd. Contour deformation is introduced by sinusoidally modulating the contour of the base circle as a function of polar angle (θ):

$$r(\theta) = r_{\text{mean}}(1 + A \sin(\omega\theta + \phi)), \quad (2)$$

where r_{mean} is the mean radius of the base circle, A is the amplitude of the sinusoidal modulation and is defined as fractional change from the mean radius at the peak, ω is the radial frequency, and ϕ is the phase of the sinusoid. Examples of the radial frequency patterns with varying amplitudes are presented in Fig. 1. In the present experiments, performance was assessed for radial frequency patterns where $\omega = 4$. We chose this radial frequency as this is the lowest radial frequency that reliably elicits optimal discrimination performance (Wilkinson et al., 1998).

All stimuli were presented on an iMac computer with a 1024×768 resolution, 75 Hz refresh rate, and 8 bit/pixel gray scale. Mean luminance was 38.0 cd/m^2 . Subjects viewed the stimuli from 1.3 m. Stimuli were generated and presented using Psychtoolbox functions (Brainard, 1997) and custom software developed in MATLAB™.

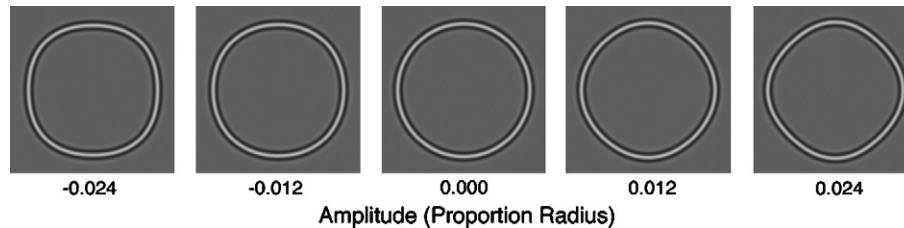


Fig. 1. Examples of the radial frequency patterns used to measure performance in the present experiments. In these examples, a negative amplitude denotes a radial frequency where $\phi = 270^\circ$, and a positive amplitude denotes a radial frequency pattern where $\phi = 90^\circ$. When the amplitude is zero, the radial frequency pattern is the base circle.

2.2. Procedure

Subjects classified the phase of the test radial frequency patterns in a two alternative forced choice procedure. For unadapted classification performance, a radial frequency pattern was presented for 53 ms in a spatial location that was randomly jittered over $3^\circ \times 3^\circ$. Adding jitter ensured that any observed after-effects could not be attributed to afterimages produced by the adapting stimuli. Following the stimulus presentation, subjects reported whether the phase of the test pattern was 90° (Fig. 1, positive amplitudes) or 270° (Fig. 1, negative amplitudes) by entering ‘1’ or ‘2’ on the keyboard. Subjects initiated the onset of the next trial by keypress. Baseline performance was measured for 13 different radial frequency amplitudes ranging from -0.012 to $+0.012$ mean radius in 0.002 increments. In this context, a reversal in sign refers to a reversal in the phase of the test radial frequency pattern.

To evaluate the effect of adaptation on classification performance, subjects adapted to a radial frequency pattern for 5 s at the onset of each trial. This length of adaptation has previously been demonstrated to be sufficient for inducing adaptation with more complex stimuli (Anderson & Wilson, 2005; Leopold et al., 2001). The same adapting shape was used throughout one experimental run. For the principal after-effect, the adapting stimulus was a high amplitude ($15\times$ threshold) pattern where $\omega = 4$. The contrast and spatial frequency of the adapting pattern were the same as the test patterns. These parameters were changed in subsequent experiments (described later) to explore the nature of these shape-specific after-effects further. Following the adaptation period, a test radial frequency pattern that was either in-phase or anti-phase to the adapting pattern was presented for 53 ms, and performance was evaluated using the same procedure described above. To adequately sample the psychometric function, the range of the 13 different radial frequency amplitudes was increased to range from -0.024 to $+0.024$ mean radius in 0.004 increments. A negative amplitude here corresponds to a stimulus that is anti-phase to the adapting pattern and a positive amplitude corresponds to a stimulus that is in-phase to the adapting pattern. Psychometric functions were measured using the method of constant stimuli, where performance for each radial frequency amplitude was measured 20 times. This resulted in 260 trials for each experimental run.

Psychometric data were fit using maximum likelihood estimation with a cumulative Gaussian function of the form

$$P(K) = \frac{1}{\sigma\sqrt{2\pi}} \int_{-\infty}^K e^{\left(\frac{-(x-\mu)^2}{2\sigma^2}\right)} dx, \quad (3)$$

where $P(K)$ refers to the proportion of times that the subject reported seeing a radial frequency pattern that was in-phase with the adapting pattern, σ refers to the standard deviation of the cumulative Gaussian function and provides a measure of slope, and μ refers to the mean of the Gaussian (50%) or the point of subjective equality (PSE). Mean psychometric performance calculated for individual subjects is based on the means and standard errors of four repetitions of each condition.

2.3. Subjects

Five subjects, three of whom were naïve to the purpose of the experiment (J.R., S.S., and Y.L.), participated in these experiments. All observers had normal or corrected to normal vision.

3. Results

3.1. Experiment 1: Opponent-shape after-effects

Classification performance for the phase of radial frequency patterns was assessed both before and after adapting to a high amplitude radial frequency pattern. For all five subjects, adapting to the radial frequency pattern resulted in a large after-effect of a radial frequency pattern 180° out of phase to the adapting pattern.

The psychometric functions for classification performance in the unadapted (solid circles) and the adapted (open circles) conditions for all five subjects are presented in Fig. 2. Performance is plotted relative to the number of times that the subject reported seeing a shape that was in-phase with the adapting pattern. As there were no biases observed for either phase in the unadapted condition, the shape considered to be the “in-phase” shape was randomized across experimental runs. Subjects were very good when classifying shape phase in the unadapted condition. The mean PSE across subjects was $0.0011(\pm 0.0011)$, which is very close to 0.0 amplitude (i.e., the base circle). Moreover, there was little variability in response, and the mean slope of the psychometric functions was remarkably steep ($\sigma = 0.0035 \pm 0.0006$). These results demonstrate that subjects were consistent and accurate when classifying opposite phases of radial frequency patterns.

The psychometric functions for the adapted condition were shifted to the right relative to the unadapted functions, indicating that subjects were more likely to report seeing the shape that was anti-phase to the adapting pattern. The mean PSE in the adapted condition was $0.0179(\pm 0.0006)$, and was significantly different from the mean PSE in the unadapted condition ($t(4) = 10.521$, $p < 0.001$). This mean PSE is approximately $3\times$ the discrimination threshold for a radial frequency pattern with these parameters (Wilkinson et al., 1998). The mean slope in the adapted condition was also reduced ($\sigma = 0.0058(\pm 0.0004)$), and was significantly different from the slope measured in the unadapted condition ($t(4) = 3.450$, $p < 0.05$). Together, these results illustrate that a strong opponent-shape after-effect can be elicited with radial frequency patterns, and that these after-effects are reflected as both a shift and a change in slope of the psychometric function.

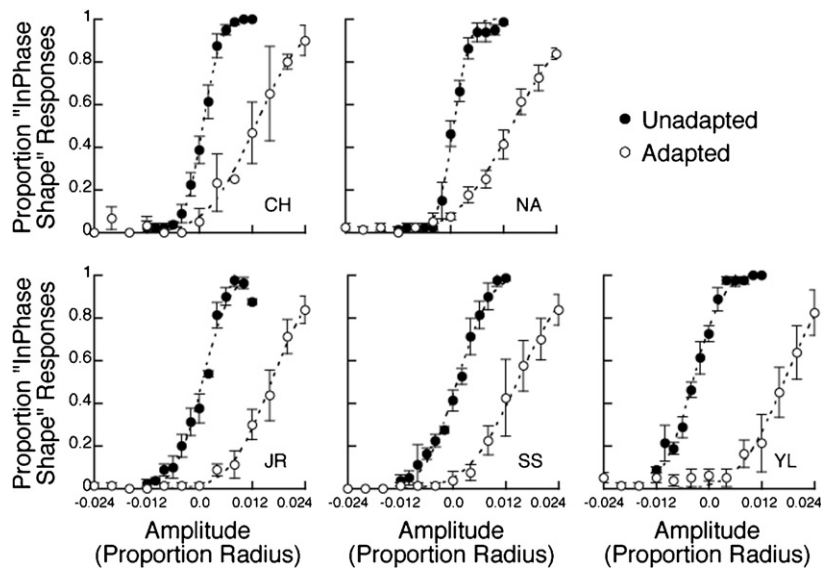


Fig. 2. Psychometric functions for classifying radial frequency phase for unadapted (closed circles) and adapted (open circles) viewing conditions. For all five subjects, adapting to a radial frequency pattern resulted in a strong shape after-effect, characterized by a shift in the function towards the anti-phase shape, and a change in slope. The dashed line represents the maximum likelihood fit of a cumulative Gaussian function.

3.2. Experiment 2: The role of contrast in shape after-effects

In an effort to determine the mechanisms that contribute to this shape after-effect, we explored classification performance under a variety of different adaptation conditions. We first wanted to determine whether or not this after-effect depended on mechanisms located beyond those in early cortical areas (i.e., V1). Contrast normalization is largely believed to be accomplished in early cortical regions, where contrast gain mechanisms have been reported (Bonds, 1989; Heeger, 1992). To establish whether the shape after-effect that we report here depends on mechanisms beyond those that are responsible for contrast gain control, we measured the strength of the shape after-effect after adapting to a low contrast (10%) stimulus (Fig. 3A). The radial frequency and size of the adapting pattern were the same as in the previous experiment. Performance was assessed using the classification procedure described above.

The results from the low contrast adaptation experiment are presented in Fig. 3. The grand psychometric functions for the unadapted, adapted (high contrast) and adapted (low contrast) conditions for all five subjects are presented in Fig. 3B, and the individual PSEs (Fig. 3C) and slope calculations (Fig. 3D) for the low contrast adapted and unadapted conditions are provided in the bottom panels. After adapting to a low contrast stimulus, the mean PSE shifted to $0.0142(\pm 0.0008)$. This mean PSE is significantly different than the mean PSE measured in the unadapted condition ($t(4) = 23.030$, $p < 0.001$; Fig. 3C), thus demonstrating that a strong and systematic after-effect can be elicited with low contrast stimuli. The slopes of the psychometric functions after adapting to a low contrast stimulus, on the other hand, were not significantly different from the unadapted slope calculations ($t(4) = 1.254$,

$p > 0.05$; Fig. 3D). Additional control experiments confirmed that adapting to a high contrast stimulus and testing with low contrast stimuli resulted in the same after-effect (data not shown). Together, these results demonstrate that the shift in the psychometric function, but not the increase in response uncertainty, can be elicited using low contrast stimuli, suggesting that the mechanisms governing the shift in the perceived shape after adaptation are located beyond those responsible for contrast gain control.

3.3. Experiment 3: Radial frequency amplitude and strength of adaptation

If the after-effect described above reflects adaptation of shape processing mechanisms, then the after-effect should also be induced with shapes that share similar geometries independent of the strength of the contour modulation. Accumulating evidence suggests that mechanisms responsible for processing shape information code shape in terms of deviation away from a mean or prototypical shape in multidimensional shape space (Kayaert, Biederman, Op de Beeck, & Vogels, 2005; Kayaert, Biederman, & Vogels, 2003; Loffler, Yourganov, Wilkinson, & Wilson, 2005). As such, shapes with the same radial frequency but that deviate more from the base circle should still induce a shape after-effect as they rely on similar processing mechanisms. We explored this possibility by adapting three subjects with radial frequency patterns that were modulated 3.25, 7.5, 15, 30, and 45 \times above threshold (Fig. 4A). All other experimental parameters were the same as those described in Section 2.

The PSEs and slopes for all three subjects with the five adapting amplitudes are presented in Figs. 4B and C, respectively. A one-way within-subjects ANOVA revealed

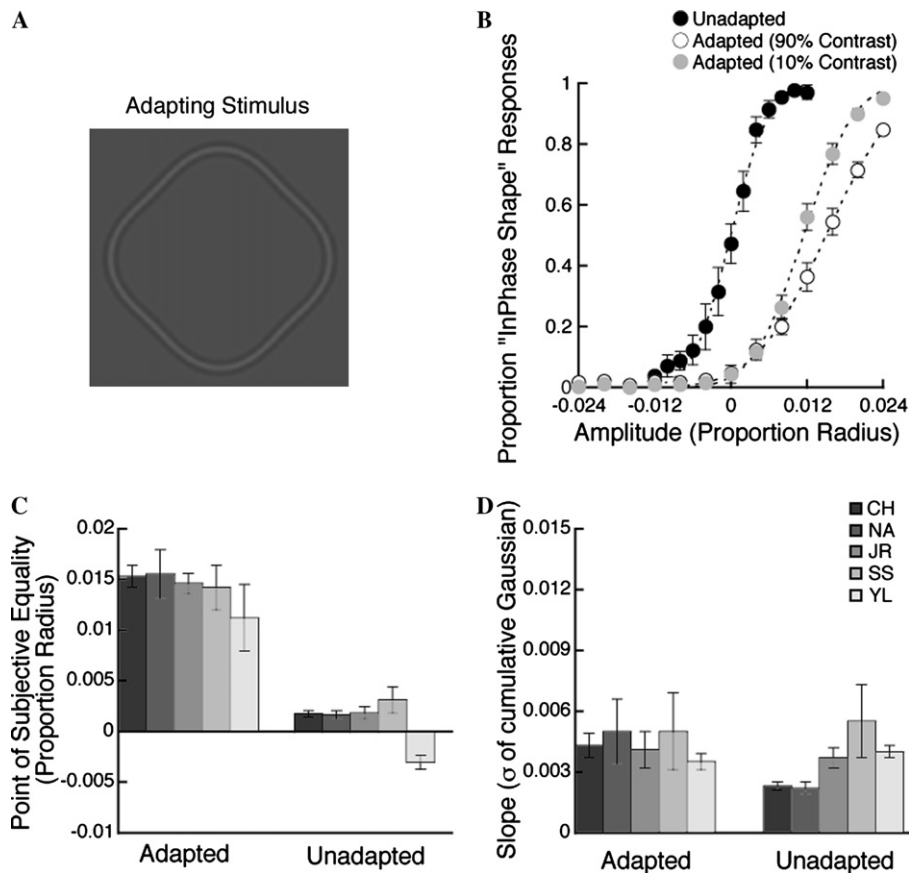


Fig. 3. Results after adapting to a low contrast radial frequency pattern. (A) An example of a low contrast (10%) adapting pattern ($\phi = 90^\circ$). (B) The grand psychometric function for five subjects after adapting to a low contrast radial frequency pattern (grey circles), compared with the grand functions from the unadapted (closed circles) and adapted (open circles) conditions (cf. Fig. 2). (C) Individual PSEs for five subjects for the low contrast adaptation (left) and unadapted (right) conditions. (D) Individual slopes of the psychometric functions for the low contrast (left) and unadapted (right) conditions.

a significant effect of adaptor amplitude on the PSE ($f_{(5,12)} = 13.026$, $p < 0.001$). Specifically, the PSEs are highest for all three subjects after adapting to the 15 \times threshold radial frequency pattern, and drop off at both lower and higher adaptor amplitudes. Nonetheless, post hoc tests revealed that at all adaptor amplitudes, the PSEs are significantly higher than the unadapted PSEs ($p < 0.01$ in each case; Fisher PLSD). A significant effect of adaptor amplitude was also observed on the slope of the psychometric function ($f_{(5,12)} = 7.311$, $p < 0.005$), with the shallowest slopes being observed after adapting to the 15 \times threshold radial frequency pattern. Unlike the PSE results, the psychometric slopes after adapting to the two lowest amplitude stimuli were not different from the unadapted condition ($p > 0.1$ in each case). The slopes after adapting to the three highest amplitudes, on the other hand, were all significantly shallower than the slopes in the unadapted condition ($p < 0.01$ in each case). Taken together, these results suggest that the change in the PSE occurs for a wide range of adaptor amplitudes, and is tuned to radial frequency amplitudes that are around 15 \times above threshold. Uncertainty, on the other hand, only increases after adapting to radial frequency patterns that are 15 \times above threshold.

3.4. Experiment 4: Contributions from local and global processing mechanisms towards shape-specific adaptation

Our claim until this point is that the after-effects that we report here reflect activity from mechanisms responsible for processing global shape information, as opposed to lower-level (i.e., local) processing mechanisms. If this shape-specific adaptation is in fact global, then the shape after-effect should transfer to forms that share the same global shape characteristics regardless of local shape characteristics. Furthermore, the after-effect should *not* transfer to forms that share local shape characteristics with no common global characteristics.

To establish whether this shape after-effect reflects adaptation of a global shape processing mechanism, we investigated whether or not the after-effect transferred over different shape sizes. Neurophysiological (Ito, Tamura, Fujita, & Tanaka, 1995; Sáry, Vogels, & Orban, 1993; Schwartz, Desimone, Albright, & Gross, 1983), neuroimaging (Grill-Spector & Malach, 2001) and behavioural (Biederman & Cooper, 1992; Jolicoeur, 1987) results suggest that the mechanisms responsible for processing global form are more size invariant than lower-level mechanisms. Size invariant adaptation effects have also been demonstrated

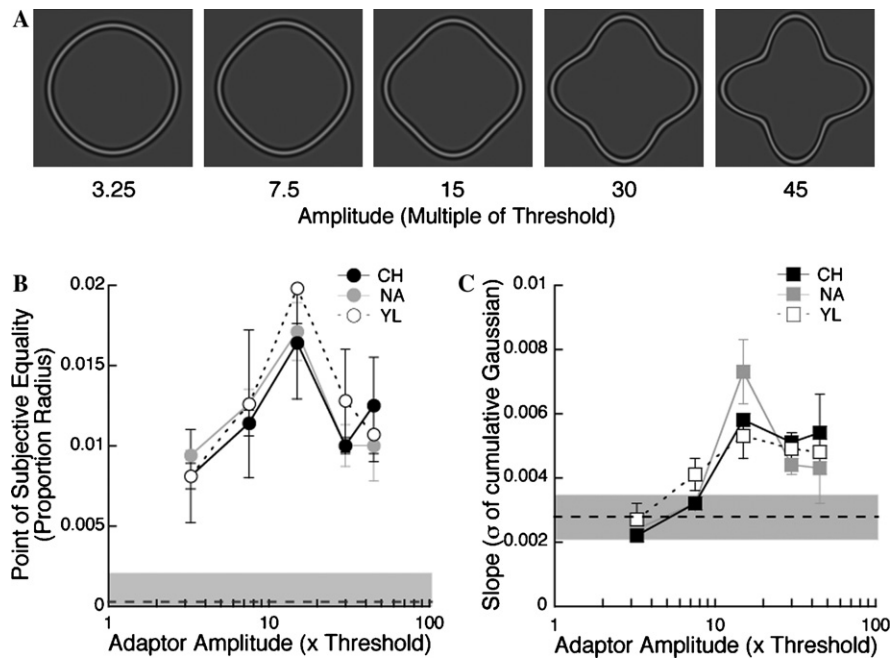


Fig. 4. The effect of adaptor amplitude on the strength of the shape after-effect. (A) Examples of the five radial frequency amplitudes used during the adapting period, defined with respect to multiple of threshold. (B) Mean PSEs for three subjects for the five adaptor amplitudes. The mean and standard error of the PSEs measured in the unadapted condition are represented by the dashed line and grey area, respectively. (C) Mean slopes of the psychometric functions for three subjects for the five adaptor amplitudes. The mean and standard error of the slopes measured in the unadapted condition are represented by the dashed line and grey area, respectively.

when adapting to other complex forms (Anderson & Wilson, 2005; Zhao & Chubb, 2001), thus suggesting that these mechanisms are indeed global in nature. In the present study, adaptation effects were measured after subjects adapted to radial frequency patterns that were scaled either $4\times$ smaller ($r = 0.5^\circ$; peak spatial frequency = 16.0 cpd) or larger ($r = 2^\circ$; peak spatial frequency = 4.0 cpd) in area than the test stimulus (Fig. 5A). All other experimental parameters were the same as those described in Section 2.

The results for five subjects after adapting to a different sized radial frequency pattern are presented in Fig. 5, where the grand psychometric functions for the unadapted, adapted (same size) and adapted (different size) are presented in Fig. 5B, and the individual PSEs (Fig. 5C) and slope calculations (Fig. 5D) for the adapted (different size) and unadapted conditions are presented in the bottom panel. After adapting to a different sized radial frequency pattern, the mean PSE shifts to $0.0096(\pm 0.0005)$. This shift in PSE is significantly different from the PSEs measured in the unadapted condition ($t(4) = 7.791$, $p < 0.005$; Fig. 5C). The slopes of the psychometric function, on the other hand, are not significantly different from the slopes measured in the unadapted condition ($t(4) = 1.010$, $p > 0.1$; Fig. 5D). Thus, the after-effect observed after adapting to a different sized stimulus can be characterized as a shift in the point of subjective equality towards the anti-phase shape with no increase in response uncertainty.

To evaluate the role of local (i.e., orientation-selective) processing mechanisms, we measured classification performance with radial frequency patterns where $\omega = 4$ after

adapting to patterns where $\omega = 5$ (Fig. 6A). Both adapting and test patterns shared the same mean radius. In this condition, the adapting and test stimuli have different global structures, but share local regions of spatially overlapping features. As such, any adaptation effects observed here will solely reflect the activity from adapted local orientation processing mechanisms. All other experimental parameters were the same as described in Section 2.

The results after adapting to a $\omega = 5$ radial frequency pattern are presented in Fig. 6, where the grand psychometric functions are presented in Fig. 6B, and the individual PSEs and slopes are presented in Figs. 6C and D, respectively. Adapting to a different radial frequency does not result in a shift in the PSE ($t(4) = 0.834$, $p > 0.1$; Fig. 6C). However, the slope of the psychometric functions are significantly shallower after adapting to the $\omega = 5$ radial frequency pattern ($t(4) = 5.883$, $p < 0.005$; Fig. 6D). Adapting to a different global shape, therefore, results in an increase in uncertainty with no shift in the point of subjective equality.

To ensure that these after-effects are specific to the global and local properties of the adapting shape as opposed to a more general nonspecific adaptation effect, subjects adapted to a radial frequency pattern that shared neither global nor local features with the test stimuli. Adapting radial frequency patterns in this condition were different sized patterns where $\omega = 5$ (Fig. 7A). As expected, neither the PSEs (Fig. 7C) nor the calculated slopes (Fig. 7D) differed from the unadapted condition (PSE: $t(4) = 0.858$, $p > 0.1$; slopes: $t(4) = 0.823$, $p > 0.1$). Taken together, then,

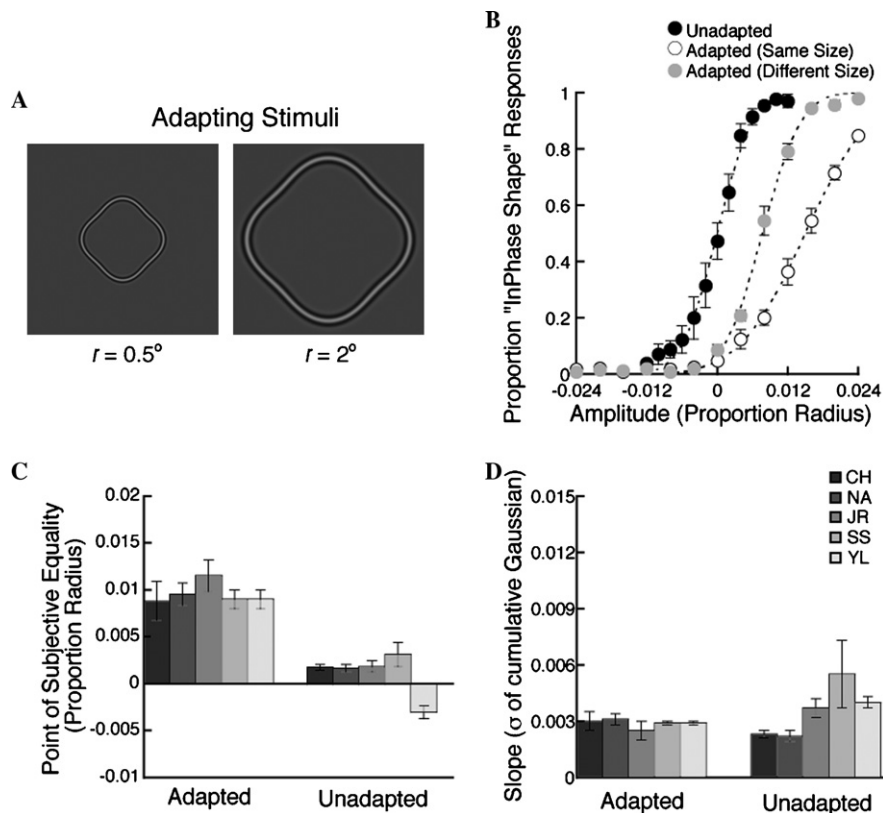


Fig. 5. Results after adapting to radial frequency patterns that were 4 \times smaller or larger in area than the test patterns. (A) Examples of both the small (left) and large (right) radial frequency patterns used during the adaptation period. (B) Grand psychometric functions after adapting to different sizes of radial frequency patterns (grey circles), compared with the grand functions from the unadapted (closed circles) and adapted (open circles) conditions. (C) Individual PSEs for five subjects for the different sized adaptation (left) and unadapted (right) conditions. (D) Individual slopes of the psychometric functions for the different sized adaptation (left) and unadapted (right) conditions. Adapting to different sizes of radial frequency patterns results in a shift of the function, but does not result in a change in slope.

these results suggest that local adaptation effects are reflected as an increase in response uncertainty, whereas global shape-specific effects are reflected as a shift in the point of subjective equality.

4. Discussion

We have demonstrated that a strong and systematic after-effect can be induced using shapes defined purely in terms of curvature deformation. This after-effect is characterized as a shift in the point of subjective equality towards a shape that is 180° out of phase with the adapting pattern, and an increase in response uncertainty (i.e., a reduction in the psychometric slope). The strength of the after-effect is consistent with a shape that is 2–3 \times above shape discrimination thresholds under these conditions. The after-effect does not depend on the contrast of the adapting stimulus and is consistent with neural mechanisms located beyond those responsible for contrast gain control. Adapting to a different sized pattern induces a perceptual shift without a reduction in slope, whereas adapting to a pattern with a different shape (i.e., radial frequency) with local overlap induces a reduction in slope without a perceptual shift. Together, these results suggest that shape after-effects

reflect dissociable contributions from both local and global processing mechanisms, where the perceived “opponent” shape largely reflects activity from mechanisms responsible for processing global shape characteristics.

The nature of the shape after-effect that we present here strongly suggests that the neural mechanisms responsible for the perceived opponent shape are located at a level of processing beyond V1. The finding that shape adaptation is largely contrast independent was first presented by Suzuki (2001), where he demonstrated that the strength of shape adaptation with hourglass contours relied on the visibility of the adaptor (i.e., contrast energy) as opposed to the contrast of the adaptor. The fact that the after-effect is largely independent of adapting contrast points to adapted mechanisms that saturate at lower contrasts. Contrast responses of neurons in IT (Rolls & Baylis, 1986) have considerably lower saturation limits than earlier visual areas (Sclar, Maunsell, & Lennie, 1990). This suggests that shape adaptation may probe higher visual cortical populations, and does not reflect any gain control mechanisms that are observed in first-order neurons. In addition to finding that low contrast adaptors could still induce an after-effect, we also found that uncertainty was reduced with lower contrast adaptors. This supports our idea that adaptation of

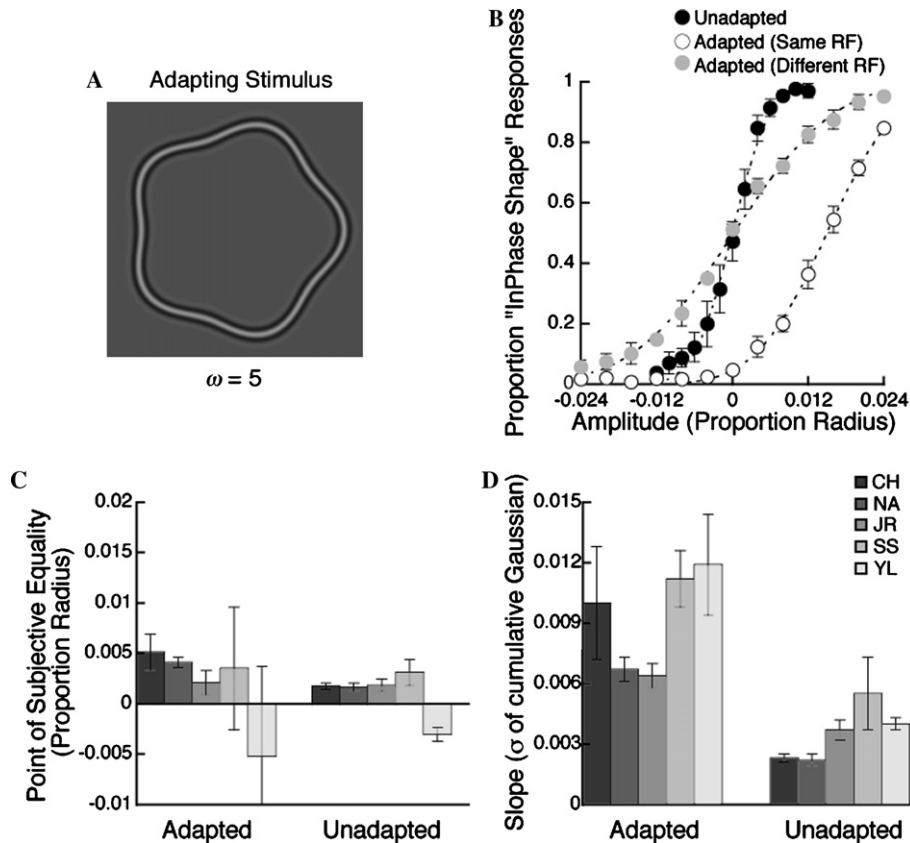


Fig. 6. Results after adapting to a different radial frequency pattern ($\omega = 5$). (A) An example radial frequency 5 pattern. All other panels and labels are the same as in Figs. 3 and 5. Performance does not shift after adapting to a different radial frequency pattern (C), but there is a reduction in the slope of the function (D).

local processing mechanisms may be represented as an increase in response uncertainty, as reducing the contrast of the adaptor should reduce the strength of adaptation (and thus the uncertainty) of V1 neurons.

We found that adapting to radial frequency patterns that shared a similar geometry but that were modulated at different amplitudes still induced a shape after-effect. This suggests a shape processing system where shape selective mechanisms respond to deviations away from the so-called mean. This idea is consistent with recent evidence in the literature that neural mechanisms selective for complex shapes respond along polar coordinates in multidimensional shape space (Kayaert et al., 2005; Kayaert et al., 2003; Loffler et al., 2005). Adapting to radial frequency patterns from an extremely wide range of amplitudes (i.e., 3.25–45 \times threshold) still induced a percept of a shape that was anti-phase to the adapting pattern. However, the strongest after-effect was elicited with a pattern that was modulated 15 \times above threshold, indicating that shape adaptation is tuned for shapes that are modulated at amplitudes that are considerably higher than threshold. This presents strong evidence that the shape after-effect we report here is not due to simple neural fatigue, as a fatigue hypothesis would predict that the strongest after-effect would be elicited with adapting amplitudes that are similar to the amplitudes of the test stimuli (i.e., less than $\sim 5\times$

threshold). Instead, these results suggest that shape after-effects reflect a more active function of cortical processing, such as some form of gain control.

Several features of the shape-selective after-effect that we report here provide strong evidence that the shift in the point of subjective equality reflects adaptation of global shape processing mechanisms as opposed to local processing mechanisms. First, we found that the adaptation effect transferred across different sizes of radial frequency patterns, providing strong evidence that the adapted mechanisms are largely size invariant and respond to global shape properties. Moreover, the adaptation effect also transfers over at least a twofold difference in spatial frequency, as the spatial frequency of the radial frequency pattern was scaled in proportion with the overall size of the pattern. Finally, a strong after-effect was elicited even though the presentation of the test pattern was always randomly jittered over a $3^\circ \times 3^\circ$ area, demonstrating at least partial position invariance of the after-effect. Size and position invariance are features of neurons located in higher cortical regions, and are thought to reflect the integration of contours processed in earlier visual areas into more complex forms (Brincat & Connor, 2004; Pasupathy & Connor, 1999, 2001). Behaviourally, then, the shift in the point of subjective equality following adaptation likely reflects activity from global shape processing mechanisms.

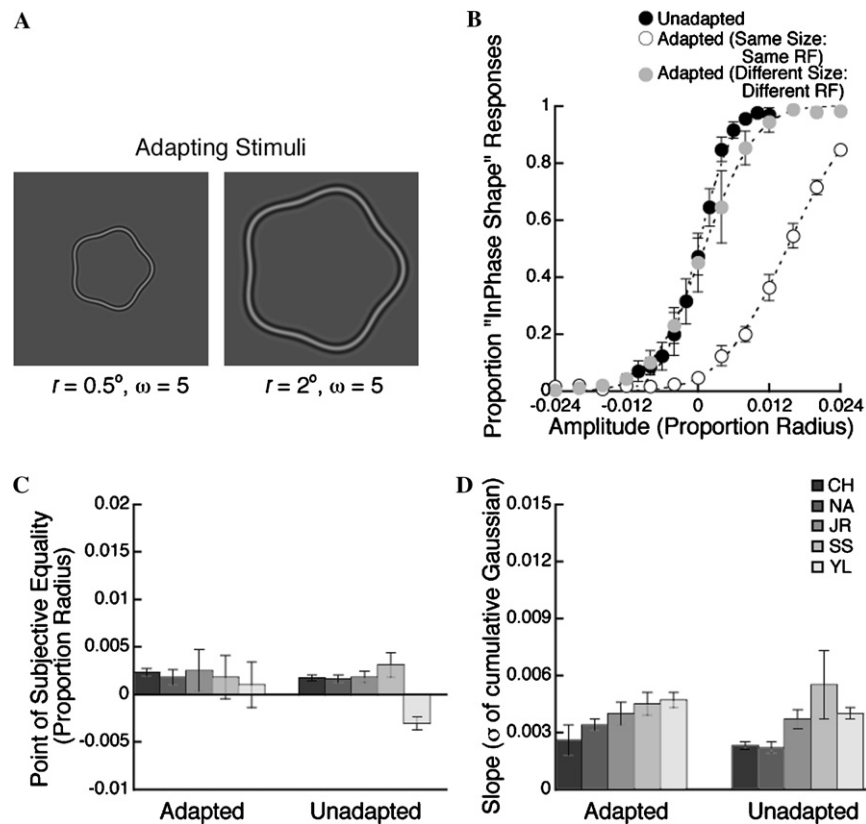


Fig. 7. Results after adapting to a pattern with a different frequency and size. Panels and labels are the same as in previous figures. Neither PSEs (C) nor slopes (D) are significantly different from unadapted after adapting to patterns that are a different frequency and size.

This finding is also consistent with other psychophysical evidence that has demonstrated that radial frequency patterns are processed by mechanisms that are sensitive to global stimulus attributes (Habak, Wilkinson, Zakher, & Wilson, 2004; Keeble & Hess, 1999; Loffler, Wilson, & Wilkinson, 2003; Wilkinson et al., 1998).

On the other hand, the shallower slopes of the psychometric functions that are observed after adapting to different radial frequency patterns likely reflect activity from orientation-selective mechanisms responsible for processing local regions of space. After adapting to a pattern with a radial frequency of 5, subjects did not systematically report seeing a shape that was different from the one presented. Instead, subjects were considerably more uncertain about the shape presented. This uncertainty may reflect noise from adapted mechanisms sensitive to local features at low and/or intermediate levels of visual processing, thereby providing a less coherent signal to higher stages of object processing. The fact that the shift in the point of subjective equality and the decision uncertainty are dissociable provides strong evidence that these behavioural manifestations arise from different neural populations.

Our results are consistent with the handful of studies that have investigated the nature of global shape adaptation, where prolonged viewing of a shape results in the percept of an opponent shape. (Suzuki & Cavanagh, 1998)

proposed that these so-called “repulsive” after-effects can be accounted for by a shift in the sensitivities of the underlying neural population code. The general principle of this model is presented in Fig. 8, where the bottom curves in each panel represent the responses from a neural population that is selective for shape with the central mechanism being most responsive to a mean circle, and the flanking mechanisms being most responsive to in-phase and anti-phase radial frequency patterns. The top curves represent the response distribution of the overall decision and are based on the strength of the output for the test pattern from the neural population. For simplicity, the schematic illustrates the population response when the test stimulus is a circle. In this model, the decision regarding the shape presented is based on the centroid of the summed population activity from shape-selective mechanisms (Fig. 8A). After adapting to a radial frequency 4 pattern, the responses for neurons responsible for processing the adapted phase will be reduced in amplitude, thereby shifting the overall decision code towards the anti-phase shape. Our results, however, would also suggest that the variance of the population code increases after adaptation, thereby increasing the uncertainty of the system response (Fig. 8B). If the bandwidths of mechanisms responsible for processing similar but adjacent shapes in shape space increase, then those mechanisms will contribute more of a response for the overall output thereby increasing the overall uncertainty

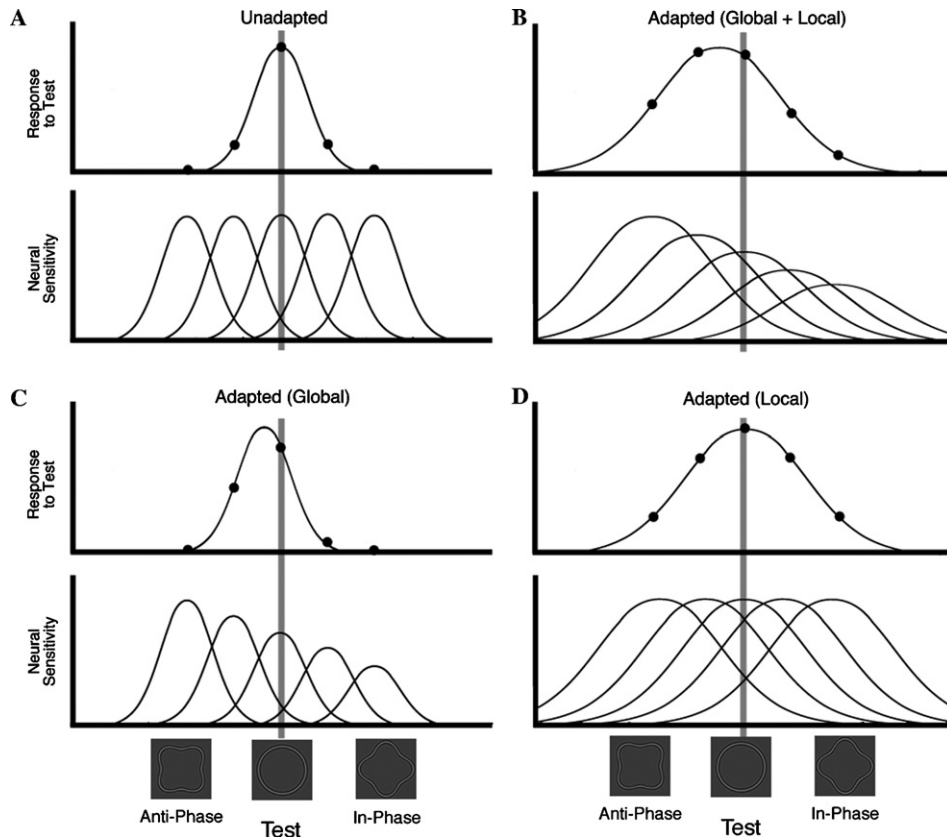


Fig. 8. Proposed model of the population response from hypothetical shape selective mechanisms under different adaptation conditions (based on (Suzuki & Cavanagh, 1998)). The overall distribution of the decision (top curves) reflect the summed neural input from shape-selective neural mechanisms (bottom curves). These are the hypothetical responses when the system is presented with a mean circle. (A) With no adaptation, the decision is based on the centroid from the weighted sum of inputs from earlier shape-selective mechanisms. (B) After adapting to a shape that is the same size and radial frequency (i.e., global and local mechanisms), the weights of the neural inputs shift towards the anti-phase shape, and increase in bandwidth (uncertainty). (C) Only adapting global shape processing mechanisms changes the strength of the input. (D) Only adapting the local processing mechanisms increases the bandwidth of the inputs.

of the decisional system. If only global shape mechanisms are adapted, the response distribution solely reflects a shift in the neural sensitivities in the population code. The bandwidths of the neural input, in this case, remain unchanged (Fig. 8C). Alternatively, adapting local contour mechanisms does not result in an overall shift in the population code (Fig. 8D). Instead, the bandwidths of the neural input increase, thereby increasing the uncertainty of the overall decision. Mechanistically, an increase in the uncertainty of the neural response could be accomplished through shape-nonspecific lateral interactions at intermediate stages of visual processing.

In summary, our results demonstrate that shape-specific after-effects can be elicited through adaptation in the curvature domain. Our results suggest that the affected neural populations are responsible for processing form and are located beyond those responsible for processing lower-level visual attributes. Moreover, these after-effects appear to reflect two types of adaptation, a shape-specific global after-effect and a nonspecific local after-effect. As these two after-effects can be demonstrated independently, this implies that they reflect two different gain controls that contribute to shape processing. Moreover, the difference

in the nature of the after-effect suggests that the mechanisms that underlie the local and global gain controls are fundamentally different from each other, and may reflect a refinement in information processing at progressive stages along the ventral processing stream.

Acknowledgments

This research is supported in part by Canadian Institutes of Health Research Training Grant in Vision Health Research, NIH Grant #EY002158 to H.R.W., NSERC Grant #OP0007551 to F.W., and a CIHR postdoctoral fellowship to C.H. Portions of these results were reported at the Vision Sciences Society meeting, May 2005.

References

- Alter, I., & Schwartz, E. L. (1988). Psychophysical studies of shape with Fourier descriptor stimuli. *Perception*, *17*, 191–202.
- Anderson, N. D., & Wilson, H. R. (2005). The nature of synthetic face adaptation. *Vision Research*, *45*, 1815–1828.
- Biederman, I., & Cooper, E. E. (1992). Size invariance in visual object priming. *Journal of Experimental Psychology: Human Perception and Performance*, *18*(1), 121–133.

- Blakemore, C., & Campbell, F. W. (1969). On the existence of neurones in the human visual system selectively sensitive to the orientation and size of retinal images. *Journal of Physiology*, 203, 237–260.
- Blakemore, C., Nachmias, J., & Sutton, P. (1970). The perceived spatial frequency shift: Evidence for frequency-selective neurones in the human brain. *Journal of Physiology*, 210(3), 727–750.
- Blakemore, C., & Sutton, P. (1969). Size adaptation: A new after-effect. *Science*, 166, 245–247.
- Bonds, A. B. (1989). Role of inhibition in the specification of orientation selectivity of cells in the cat striate cortex. *Visual Neuroscience*, 2(1), 41–55.
- Brainard, D. H. (1997). The psychophysics toolbox. *Spatial Vision*, 10, 433–436.
- Brincat, S. L., & Connor, C. E. (2004). Underlying principles of visual shape selectivity in posterior inferotemporal cortex. *Nature Neuroscience*, 7(8), 880–886.
- Campbell, F. W., & Maffei, L. (1971). The tilt after-effect: A fresh look. *Vision Research*, 11, 833–840.
- Desimone, R., & Schein, S. J. (1987). Visual properties of neurons in area V4 of the macaque: Sensitivity to stimulus form. *Journal of Neurophysiology*, 57, 835–868.
- DeValois, R. L., & DeValois, K. K. (1988). *Spatial vision*. New York: Oxford University Press.
- Gallant, J. L., Braun, J., & Van Essen, D. C. (1993). Selectivity for polar, hyperbolic, and Cartesian gratings in macaque visual cortex. *Science*, 259(5091), 100–103.
- Gallant, J. L., Connor, C. E., Rakshit, S., Lewis, J. W., & Van Essen, D. C. (1996). Neural responses to polar, hyperbolic, and Cartesian gratings in area V4 of the macaque monkey. *Journal of Neurophysiology*, 76(4), 2718–2739.
- Gibson, J. J. (1933). Adaptation, after-effect and contrast in the perception of curved lines. *Journal of Experimental Psychology*, 16, 1–31.
- Gibson, J. J., & Radner, M. (1937). Adaptation, after-effect and contrast in the perception of tilted lines. I. Quantitative studies. *Journal of Experimental Psychology*, 20, 453–467.
- Greenlee, M. W., & Heitger, F. (1988). The functional role of contrast adaptation. *Vision Research*, 28(7), 791–797.
- Grill-Spector, K., & Malach, R. (2001). fMR-adaptation: A tool for studying the functional properties of human cortical neurons. *Acta Psychologica*, 107, 293–321.
- Habak, C., Wilkinson, F., Zakher, B., & Wilson, H. R. (2004). Curvature population coding for complex shapes in human vision. *Vision Research*, 44(24), 2815–2823.
- Heeger, D. J. (1992). Normalization of cell responses in cat striate cortex. *Visual Neuroscience*, 9(2), 181–197.
- Hubel, D. H., & Wiesel, T. N. (1968). Receptive fields and functional architecture of monkey striate cortex. *Journal of Physiology (London)*, 195, 215–243.
- Ito, M., Tamura, H., Fujita, I., & Tanaka, K. (1995). Size and position invariance of neuronal responses in monkey inferotemporal cortex. *Journal of Neurophysiology*, 73(1), 218–226.
- Jolicoeur, P. (1987). A size-congruency effect in memory for visual shape. *Memory and Cognition*, 15(6), 531–543.
- Kayaert, G., Biederman, I., Op de Beeck, H. P., & Vogels, R. (2005). Tuning for shape dimensions in macaque inferior temporal cortex. *European Journal of Neuroscience*, 22, 212–224.
- Kayaert, G., Biederman, I., & Vogels, R. (2003). Shape tuning in macaque inferior temporal cortex. *Journal of Neuroscience*, 23, 3016–3027.
- Keeble, D. R. T., & Hess, R. F. (1999). Discriminating local continuity in curved figures. *Vision Research*, 39, 3287–3299.
- Kobatake, E., & Tanaka, K. (1994). Neuronal selectivities to complex object features in the ventral visual pathway of the macaque cerebral cortex. *Journal of Neurophysiology*, 71(3), 856–867.
- Kohler, W., & Wallach, H. (1944). Figural after-effects. An investigation of visual processes. *Proceedings of the American Philosophical Society*, 88(4), 269–357.
- Leopold, D. A., O'Toole, A. J., Vetter, T., & Blanz, V. (2001). Prototype-referenced shape encoding revealed by high-level after-effects. *Nature Neuroscience*, 4(1), 89–94.
- Loffler, G., Wilson, H. R., & Wilkinson, F. (2003). Local and global contributions to shape discrimination. *Vision Research*, 43, 519–530.
- Loffler, G., Yourganov, G., Wilkinson, F., & Wilson, H. R. (2005). fMRI evidence for the neural representation of faces. *Nature Neuroscience*, 8(10), 1386–1390.
- Pantle, A., & Sekuler, R. (1968). Size-detecting mechanisms in human vision. *Science*, 162(858), 1146–1148.
- Pasupathy, A., & Connor, C. E. (1999). Responses to contour features in macaque area V4. *Journal of Neurophysiology*, 82(5), 2490–2502.
- Pasupathy, A., & Connor, C. E. (2001). Shape representation in area V4: Position-specific tuning for boundary conformation. *Journal of Neurophysiology*, 86(5), 2505–2519.
- Regan, D., & Hamstra, S. J. (1992). Shape discrimination and the judgement of perfect symmetry: Dissociation of shape from size. *Vision Research*, 32(10), 1845–1864.
- Rolls, E. T., & Baylis, G. C. (1986). Size and contrast have only small effects on the responses to faces of neurons in the cortex of the superior temporal sulcus of the monkey. *Experimental Brain Research*, 65(1), 38–48.
- Sáry, G., Vogels, R., & Orban, G. A. (1993). Cue-invariant shape selectivity of macaque inferior temporal neurons. *Science*, 260, 995–997.
- Schwartz, E. L., Desimone, R., Albright, T. D., & Gross, C. G. (1983). Shape recognition and inferior temporal neurons. *Proceedings of the National Academy of Sciences of the United States of America*, 80, 5776–5778.
- Scarl, G., Maunsell, J. H. R., & Lennie, P. (1990). Coding of image contrast in central visual pathways of the macaque monkey. *Vision Research*, 30(1), 1–10.
- Suzuki, S. (2001). Attention-dependent brief adaptation to contour orientation: A high-level after-effect for convexity? *Vision Research*, 41, 3883–3902.
- Suzuki, S. (2003). Attentional selection of overlapped shapes: A study using brief shape after-effects. *Vision Research*, 43, 549–561.
- Suzuki, S., & Cavanagh, P. (1998). A shape-contrast effect for briefly presented stimuli. *Journal of Experimental Psychology: Human Perception and Performance*, 24(5), 1315–1341.
- Webster, M. A. (2004). Pattern-selective adaptation in color and form perception. In L. M. Chalupa & J. S. Werner (Eds.), *The visual neurosciences* (pp. 936–947). Cambridge: The MIT Press.
- Wilkinson, F., Wilson, H. R., & Habak, C. (1998). Detection and recognition of radial frequency patterns. *Vision Research*, 38, 3555–3568.
- Wilson, H. R., & Humanski, R. (1993). Spatial frequency adaptation and contrast gain control. *Vision Research*, 33(8), 1133–1149.
- Zhao, L., & Chubb, C. (2001). The size-tuning of the face-distortion after-effect. *Vision Research*, 41(23), 2979–2994.